Landau theory and phase diagram of $KMn_{1-x}Ca_xF_3$ ferroelastic crystal near the tricritical point: calorimetric and order parameter study

2004 J. Phys.: Condens. Matter 16 2879

(http://iopscience.iop.org/0953-8984/16/16/012)

INSTITUTE OF PHYSICS PUBLISHING JOURNAL OF PHYSICS: CONDENSED MATTER

J. Phys.: Condens. Matter **16** (2004) 2879–2890 PII: S0953-8984(04)75832-4

Landau theory and phase diagram of $KMn_{1-x}Ca_xF_3$ ferroelastic crystal near the tricritical point: calorimetric and order parameter study

F J Romero[1], M C Gallardo[1], S A Hayward[2], J Jiménez[1], J del Cerro[1] and E K H Salje[2]

[1] Departamento de Física de la Materia Condensada, Universidad de Sevilla, PO Box 1065, E-41080 Sevilla, Spain
[2] Department of Earth Sciences, University of Cambridge, Downing Street, Cambridge CB2 3EQ, UK

E-mail: fjromero@us.es

Received 2 February 2004
Published 8 April 2004
Online at stacks.iop.org/JPhysCM/16/2879
DOI: 10.1088/0953-8984/16/16/012

Abstract

The cubic to tetragonal phase transition in the solid solution $K(Mn, Ca)F_3$ has been investigated by conduction calorimetry and x-ray diffraction. The behaviour of the excess specific heat, latent heat and spontaneous strain has been explained in terms of a 2–4–6 Landau potential. The coefficients A and C, prefactors of Q^2 and Q^6 in the free energy expansion, are practically constant with composition, but B (the prefactor of Q^4) and T_C are functions of composition. The tricritical point occurs when the sign of B changes from negative (in pure $KMnF_3$) to positive (in Ca rich samples). However, the variation of the parameters B and T_C with dopant concentration x is non-linear. The dependence of T_C with composition is explained in terms of an internal stress due to the doping ion of Ca and is compared with the effect of external uniaxial stress on pure $KMnF_3$.

1. Introduction

Potassium manganese fluorite, $KMnF_3$, undergoes a ferroelastic phase transition, analogous to the transition in $SrTiO_3$, from the cubic perovskite structure to a tetragonal structure at 186 K [1]. This phase transition is discontinuous but close to a tricritical point [2, 3]. In a previous paper we evaluated the latent heat to be $L = 19.5(3)$ J mol^{-1} [4]. We have also shown that the transition can be described using a 2–4–6 Landau potential, $\Delta G = \frac{1}{2}A(T - T_C)Q^2 + \frac{1}{4}BQ^4 + \frac{1}{6}CQ^6$, whose coefficients have been determined experimentally [5].

The first order character of this phase transition can be changed by the effect of the uniaxial stress (σ) or compositional substitution. Stokka *et al* [6, 7] measured the thermal hysteresis

of the specific heat under uniaxial stress. They reported the existence of a tricritical point near $\sigma = 0.45$ kbar with σ along [110] and the existence of two consecutive tricritical points joined by a second order line near $\sigma = 0.25$ kbar with σ along [100]. In the phase diagram T_{max} versus σ, for a uniaxial stress along [110], two distinct regimes exist; for stresses lower than the tricritical point, σ^* (first order phase transitions), the slope $dT_{max}/d\sigma$ is greater than for stresses higher than σ^* (second order phase transitions). They compare this result with the similar one obtained previously for $RbCaF_3$ under uniaxial stress [8].

Also a similar behaviour has been calculated within molecular-field theory for the [111] stress induced tricritical point for the ferromagnetic phase transition in MnO [9].

As well as the effect of externally applied stress, various ionic substitutions also modify the phase transition [10–15]. One of the most interesting cases is the solid solution obtained with the substitution of Mn by Ca in $KMn_{1-x}Ca_xF_3$. The addition of Ca^{2+} impurities increases the transition temperature and shifts the transition to second-order [10, 11, 13]. It has been argued that the relevant defect is not simply a Ca^{2+} ion but a more extended defect configuration. As Ca^{2+} ions are much bigger than Mn^{2+} ions, they act on the (Ca, Mn)–F bonds in a similar way to a stress along the $\langle 001 \rangle$ directions of the cubic phase.

Gibaud *et al* [13] argued that if there were a random distribution of Ca^{2+} defects throughout a crystal, defects would act as a hydrostatic pressure. Nevertheless, they also suggested that the Bridgman method of crystal growth might lead to a gradient of chemical composition in a specific direction that broke the symmetry. However, in this case the doping effect would be similar to that expected from a uniaxial stress applied along the growth axis, rather than a hydrostatic pressure.

On the other hand, the behaviour of dilute (as opposed to more concentrated) solid solutions also needs special consideration. When the solute concentration is high a homogeneous chemical mixing model generally describes such systems well. This leads to composition-dependent parameters having a linear dependence on x, for example,

$$T_c = T_{c0} + \lambda x. \tag{1}$$

In the case of dilute systems, on the other hand, the behaviour of the material as a function of composition will depend also on the finite length scale of the structural relaxation around the dopant atoms, and the tendency of solute atoms to attract or repel each other. Salje [16] describes the cases of strong solute—solute attraction (leading to clustering) and strong solute—solute repulsion (leading to a widely separated solute distribution) as two limiting solutions of a single model.

If the solute atoms form clusters, additional solute atoms will tend to cause existing clusters to grow, rather than nucleating new ones. In this case, $\Delta T_C \propto x^{4/3}$, and a strong plateau will be seen; T_C will depend only weakly on x for small values of x. If, on the other hand, solute atoms repel each other, $\Delta T_C \propto x^{2/3}$, and an inverse plateau will be seen; changes in x will have a stronger effect on the phase transition for small values of x than in the homogeneous chemical mixing regime. Inverse plateaus are seen experimentally in the phase diagrams of $K_{1-x}(NH_4)_xH_2PO_4$ and $KH_2P_{1-x}As_xO_4$ [17].

In the intermediate case, ΔT_C is proportional to x, though not necessarily with the same proportionally constant seen in the chemical mixing regime. Indeed, given that a small solute concentration will leave most of the sample volume almost totally unaffected, it is intuitive to assume that the plateau regime for a random solute distribution will be characterized by T_C being almost (perhaps completely) independent of x. This behaviour has been observed in a number of systems, including $PbZr_xTi_{1-x}O_3$ [18, 19] and the mineral anorthoclase [20].

Irrespective of the behaviour of the system in the dilute regime, there is eventually a crossover to simple chemical mixing. This occurs when the distortion fields around individual

solute atoms (or clusters of solute atoms) coalesce. Where each defect is a single solute atom, the composition of the dilute regime/chemical mixing crossover, x_C, will furnish a value of the relaxation lengthscale; a typical cusp extending to $x_C = 1\%$ implies a defect cloud volume of 100 unit cells, or a radius of approximately 3 lattice repeats. If solute atoms cluster, a calculation of this radius based on x_C will tend to underestimate the radius somewhat. However, unless the system is in the strong clustering/strong plateau regime, this error is unlikely to be great.

In a previous paper we have confirmed, by measuring the specific heat and the latent heat, that the effect of the Ca is to shift the character of the transition to second order [4, 21]. We have also described the transition for the doping concentrations $x = 0.3\%$ and 2.3% by means of a 2–4–6 Landau potential whose coefficients have also been determined [22]. The analysis showed that the fourth order coefficient and T_C change strongly with the calcium concentration.

In this paper we report a systematic study of the solid solution $KMn_{1-x}Ca_xF_3$ (with $x = 0$, 0.3%, 1.7%, and 2.3%), and its analysis in terms of Landau theory. To study this solid solution we have carried out calorimetric and x-ray diffraction measurements. We have determined the effect of x on Landau free energy coefficients and we compared the phase diagram T_C versus x with the phase diagram T_C versus uniaxial stress (σ) for pure $KMnF_3$ as obtained by Stokka *et al* [6].

2. Experimental details

2.1. Sample characteristics

The samples of $KMn_{1-x}Ca_xF_3$ were provided by the University of Maine (Le Mans, France). They were prepared by the Bridgman–Stockbarger method. The resulting crystals were approximately cylindrical, with a thickness of 5 mm and circular (001) faces.

The chemical characteristics of the samples were examined using an electron microprobe CAMECA SX50. The pure $KMnF_3$ sample did not show any trace of calcium. The doped samples showed Ca concentrations of $x = 0.3$ mol%, 1.7% and 2.3%. The microanalysis experiments showed slight inhomogeneities in the composition of the doped samples; for example, the composition of the fourth sample is $2.30\% \pm 0.13\%$. We will argue that this inhomogeneity plays an important role in the behaviour of these crystals around the transition temperature.

2.2. Experimental methods

The measurements of specific heat and latent heat were performed by a high-resolution conduction calorimeter [23]. The experimental system uses the conduction calorimetry method described fully elsewhere [24]. The sample is pressed between two identical heat fluxmeters, each made from 50 chromel–constantan thermocouples [25] connected in series with wires placed in parallel lines. Using this method it is possible to obtain absolute values of specific heat.

In addition, the heat flux exchanged by the sample, which gives the total enthalpy change during the transition, was measured on the same apparatus using a technique analogous to differential thermal analysis (DTA) [4, 26]. It is also important to note that the system measures the heat flux and the specific heat in independent experiments, but using the same calorimeter and sample, and under similar thermal conditions. As a result, the specific heat and heat flux measurements are directly comparable.

Combining these two experiments we can evaluate the part of the total enthalpy that corresponds to the variation of specific heat with temperature, and separate it from the part of the enthalpy that corresponds to the latent heat. This analysis is important when the specific

Table 1. Latent heat (L) and temperature of the specific heat maximum (T_{max}) as a function of Ca concentration.

Composition (mol% Ca)	T_{max} (K)	L (J mol^{-1})
0	185.95	19.5(2)
0.30	189.72	1.5(8)
1.70	197.33	0
2.30	200.38	0

heat is very high around the transition temperature and the latent heat is small, as occurs in phase transitions near to the tricritical point, as studied in this work.

The experimental system changes the sample temperature at an extremely slow rate (typically 0.1 K h^{-1}), so that the sample is kept practically in equilibrium. We have a specific heat data point every 0.04 K, so the excess of entropy obtained from the integration of C_P data has no experimental statistical errors.

The order parameter may, in principle, be measured using a very wide range of techniques. A particularly convenient method is to determine the spontaneous strain associated with the transition. Where single crystal samples are available (as is the case in $KMnF_3$), strain data may be obtained using x-ray diffraction, using the rocking curve technique. This is described in detail elsewhere [27]. The relationship between Q and the spontaneous strain depends on the symmetry properties of the transition. In the case of the $Pm3m$–$I4/mcm$ transition in this perovskite, the spontaneous strain ε_S is proportional to Q^2.

3. Results and discussion

The order of the transition was characterized by measuring the latent heat using the method previously described. The analysis has been reported previously [4, 21] and the results are summarized in table 1. The effect of the Ca substitution is to decrease the value of the latent heat and, hence, to make the transition second order. The addition of 0.3% Ca reduces the latent heat to less than 10% of its value in pure $KMnF_3$. No latent heat was found for the 1.7% and 2.3% doped crystals. The values of the latent heat indicate that the sample with $x = 0.3\%$ is close to the tricritical point.

The specific heat data for the four samples are shown in figure 1 over a wide temperature range. At high temperatures (cubic phase) the specific heat of each sample shows a linear temperature dependence. All samples show an anomaly in the specific heat related with the cubic–tetragonal phase transition. The temperature at which the maximum of the specific heat is obtained, T_{max}, also increases with the calcium concentration (table 1). For the three Ca doped samples, the T_{max} versus x graph is practically linear with approximately 5.3 K/% Ca as the slope. However, the value of T_{max} for pure $KMnF_3$ lies around 2 K below this straight line.

The qualitative shapes of specific heat curves for the two samples showing a first order transition, pure $KMnF_3$ and $KMnF_3$ with 0.3% Ca, are similar. Both show a sharp anomaly and a relatively insignificant tail above the transition point. However, the 1.7% and 2.3% doped samples show a much more rounded peak and the transition is smeared over a wider temperature interval, with a significant tail of excess specific heat above the transition point.

This tail is probably due to the heterogeneity of the sample composition in the more highly doped samples. Combining the slope of T_{max} versus x and the variation in composition for the sample with 2.3% Ca, we estimate that the width of the transition for this sample is about 1.3 K, which agrees well with the width of specific heat around the transition temperature.

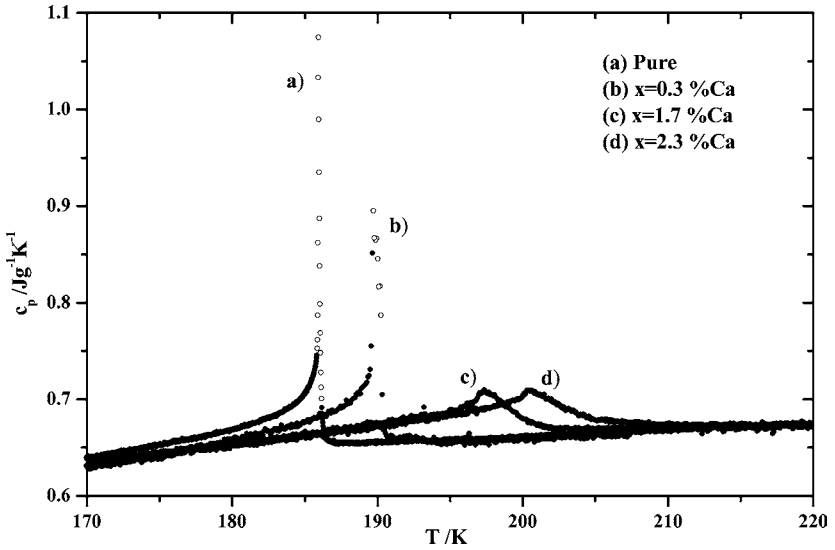

Figure 1. Experimental specific heat versus temperature for various compositions of $KMn_{1-x}Ca_xF_3$. Only filled circles represent specific heat data in the monophasic state.

Table 2. Landau coefficients for each sample of $KMn_{1-x}Ca_xF_3$.

Sample (% of Ca)	A (J K^{-1} mol^{-1})	B (J mol^{-1})	C (J mol^{-1})	T_C (K)
0	2.78(1)	−57.4(6)	573(40)	185.76(1)
0.3	2.9(2.2)	−6(4)	500(400)	190.13(1)
1.7	2.87(1)	20(5)	540(40)	200.16(1)
2.3	2.79(1)	24(5)	540(40)	202.98(1)

On the other hand, the specific heat data obtained in the temperature interval where the latent heat is produced (coexistence of phases interval) are not reliable data, because they do not correspond to data in the monophasic state. These data are represented by open circles in figure 1. Only the data represented by filled circles in figure 1 are data that represent the specific heat when the sample is in the monophasic state (para or ferro phase), and these are the data that we will consider in the analysis of the specific heat curves.

In order to analyse theoretically these phase transitions we have fitted the experimental data for each sample to a 2–4–6 Landau potential,

$$G = \frac{A}{2}(T - T_C)Q^2 + \frac{B}{4}Q^4 + \frac{C}{6}Q^6, \tag{2}$$

whose coefficients for each sample are summarized in table 2. It should be noted that the error for the sample of 0.3% are bigger than the others; this is due to the error of L and the covariance in the errors that exist between the parameters.

We observe that the sign of B changes at a composition slightly larger than 0.3%. Thus the fraction of Ca doping for which this transition passes through the tricritical point (x^*) is slightly higher than 0.3%.

The next step is to compare the $Q(T)$ behaviour predicted by the fitted potential with independent measurements of the order parameter made by another technique, such as the spontaneous strain, proportional to the twin angle measured by x-ray diffraction. Figures 2(a)–(c) show the good agreement between the experimental order parameter, obtained using

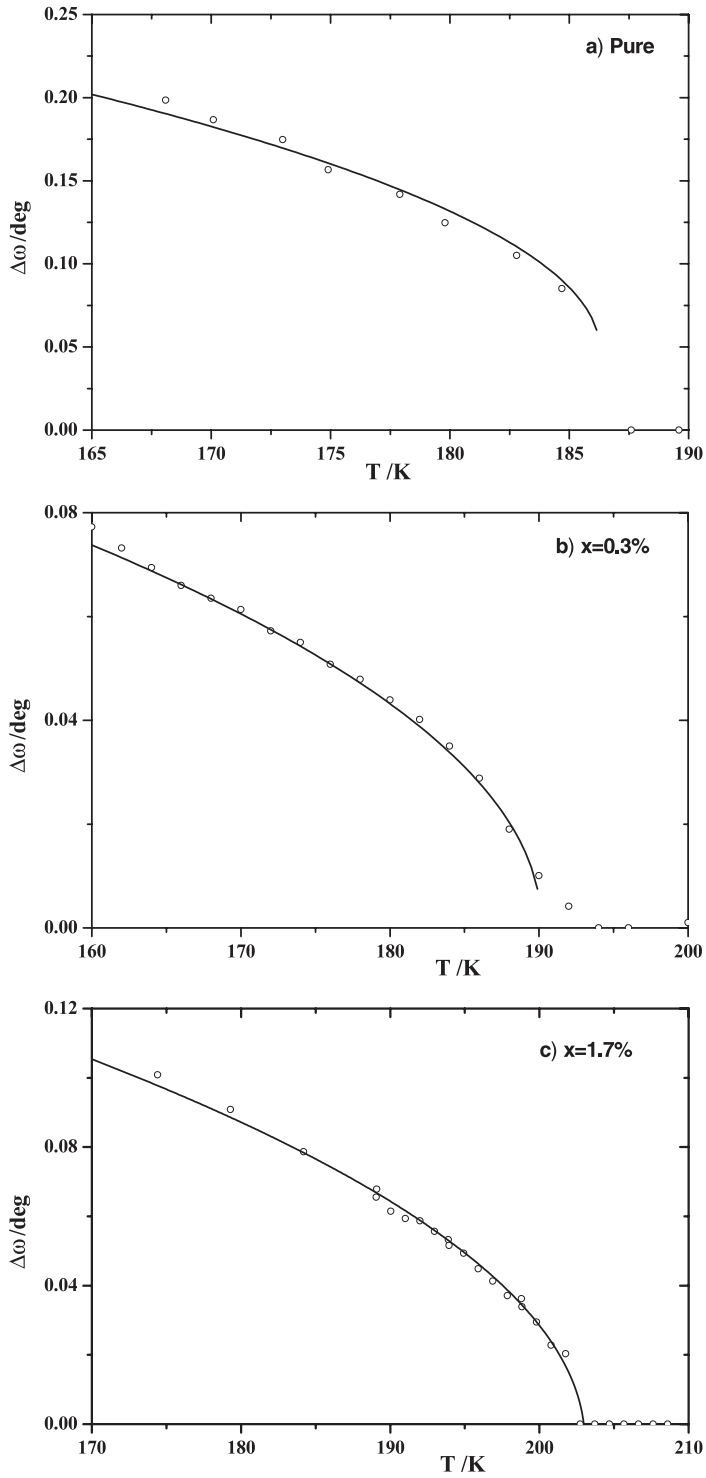

Figure 2. Comparison of the twin angle (proportional to Q^2) with the theoretical order parameter behaviour derived from the Landau potential determined from the calorimetric data for various compositions of $KMn_{1-x}Ca_xF_3$.

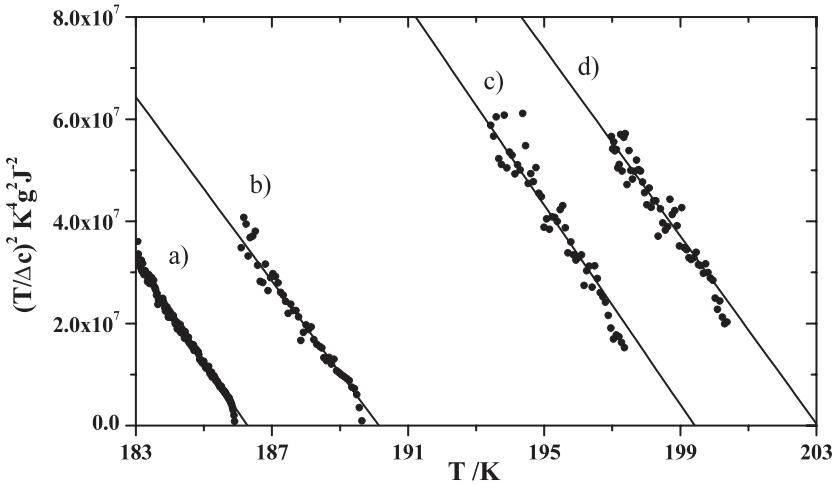

Figure 3. $(T/\Delta c_P)^2$ versus temperature for each sample. This function is expected to be linear for a phase transition described by Landau theory.

strain data and the equilibrium behaviour predicted from the Landau potential fitted using calorimetric data. The scaling between the twin angle and the order parameter was taken as an additional fitting parameter. This agreement justifies the use of Landau theory to describe these transitions. Also, according to Landau theory, we can see in figure 1 (filled circles) that the specific heat maximum increases with Ca concentration until the tricritical concentration; higher concentrations make the maximum of specific heat decrease.

The results in table 2 show that A and C do not change significantly. We can check this further by analysing the detailed behaviour of the specific heat. In a phase transition where the excess free energy is described by equation (2), the excess specific heat Δc is given by

$$\left(\frac{T}{\Delta c}\right)^2 = \frac{16A^3}{C}(T_2 - T) \qquad \text{where } T_2 = T_c + \frac{B^2}{4AC}.$$

Thus graphs of $(T/\Delta c)^2$ against temperature should be linear, with the same gradient for each sample. Figure 3 shows that these slopes are, within experimental uncertainties, the same for all four experimental curves.

Meanwhile B, T_C and T_{max} are strongly dependent on the degree of Ca doping. If we plot B and T_{max} versus x, as in figure 4, we can also see that the behaviour is clearly non-linear; all these quantities increase more rapidly for small x (where the transition is first order), than for larger x (where the transition is second order). However, the precise form of this crossover, and the composition at which it happens, are not fully constrained by these results. Measurements on samples at several additional compositions would be needed to determine these details.

Non-linear variations of T_C have also been found in the phase diagram of T_C versus uniaxial stress (σ) for a number of perovskite materials. In fact for $RbCaF_3$ under uniaxial stress a change in the T_C versus σ gradient occurs unambiguously at the tricritical point [8].

To compare the effects of doping with Ca and uniaxial applied stress in $KMnF_3$, we follow a method similar to the analysis of $Pb(Zr_xTi_{1-x})O_3$ by Rossetti *et al* [28]. Figure 5(a) shows the variation of T_{max} with the dopant concentration x from our data. The equivalent graph figure 5(b) shows the change in T_{max} with [110] stress, as measured by Stokka and Fossheim [7].

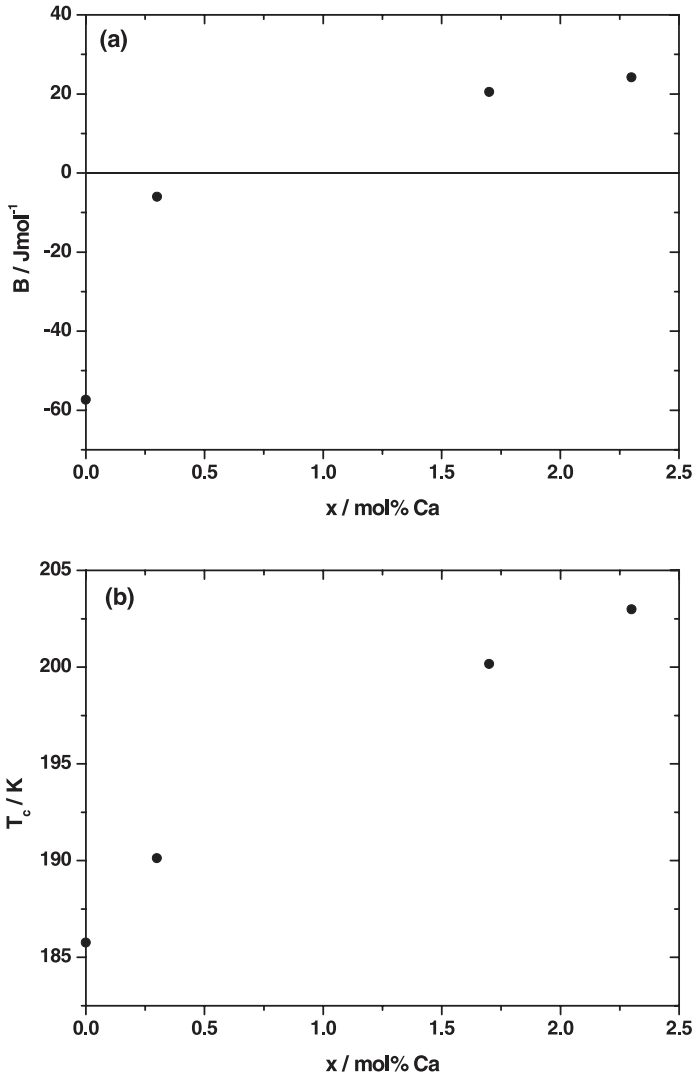

Figure 4. Variation of Landau coefficients (a) B and (b) T_C with composition in $KMn_{1-x}Ca_xF_3$.

Stokka *et al* [6, 7] measured the specific heat as a function of temperature under uniaxial stress. From these measurements, they determined the temperature of the specific heat maximum, which they labelled T_C, and the width of the thermal hysteresis, ΔT_C. Since the T_C in the Landau potential is not, in general, identical to the temperature of the specific heat maximum, we describe the temperature of the specific heat maximum as T_{max} in this report.

Both graphs, figures 5(a) and (b) show a change in slope at the tricritical point ($x \approx 0.3$ mol% for Ca doping, $\sigma = 0.45$ kbar for [110] stress), but that for chemical doping is much more pronounced.

In figure 5(c), we renormalize the two applied variables (Ca doping and [110] stress) to their values at the tricritical point. This figure shows that the changes in T_{max} caused by forcing the transition to the tricritical point are equal, whether the tricritical point is due

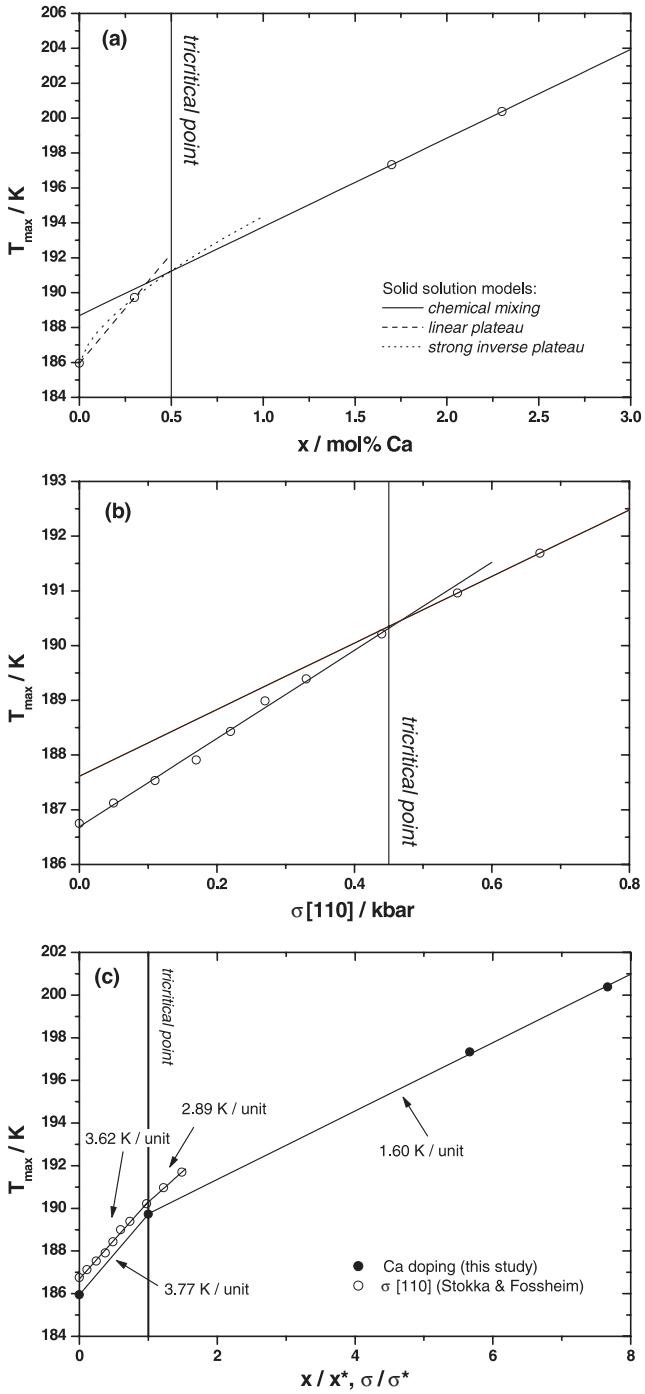

Figure 5. (a) Variation in the temperature of the c_P maximum with Ca doping in $KMnF_3$. The fit lines show the different behaviours of the plateau regime (broken and dotted curves for linear and cusp-like plateaux, respectively) and the chemical mixing regime (solid line). (b) Variation in the temperature of the c_P maximum with stress along [110], showing different gradients above and below the tricritical point. In part (c), the two applied variables are both normalized to have value 1 at the tricritical point.

to stress or Ca doping. This indicates an underlying similarity about the effects of these two external variables. On the other hand, the two curves are not identical, unlike the case of $Pb(Zr_xTi_{1-x})O_3$ [28]. The likely reason for this is that the effect of Ca doping is not proportional to the quantity of dopant; small concentrations of Ca have a greater effect than larger concentrations. This behaviour is consistent with the inverse plateau model of dilute solid solutions. However, it is not possible to study the detailed form of the cusp with the available data; more samples with different compositions in the range $x < 1\%$ would be needed for this. As a result, we can neither confirm nor rule out the theoretical prediction [16] that the exact form of the cusp is $\Delta T_C \propto x^{2/3}$.

Neither are we able to determine a precise value of the critical composition for the crossover between the inverse plateau and chemical mixing regimes. Using the data in figure 5(a), and making the rather simplistic assumption that T_{max} is linear with x in both regimes, the critical composition is $x = 0.35$ mol% Ca. Using the inverse plateau model to describe the Ca-poor solid solution, the crossover occurs at $x = 0.5$ mol% Ca. However, both these estimates are problematic, since the form of the $T_{max}(x)$ lines for both the chemical mixing and dilute regimes are determined by only two data points.

Using $x = 0.5\%$ as an upper limit for the critical composition, we may estimate a lower limit on the lengthscale of the distortion cloud surrounding each defect in $KMnF_3$ perovskite. This distortion cloud has a volume of at least 200 unit cells, and so its radius is at least of the order of 3.5–4 unit cells, or $r_C \approx 15$ Å. Given that an inverse plateau is observed, it is likely that the defects (that is, the solute atoms) are repelling each other, so cluster formation is unlikely, at least as an equilibrium phenomenon. Any clusters that did form, however, imply that the radius of the distortion field around each defect was even larger.

From the form of the phase diagram in the $K(Mn, Ca)F_3$ system, we have shown that individual Ca defects have rather long-range interactions, and that they tend to repel each other. These interactions are probably of an elastic nature. The local crystal structure of these defects has been studied directly by diffuse x-ray diffraction methods [29]. These results are consistent with the observation of a tail in the measurements of the specific heat, which is particularly pronounced in the 2.3% Ca doped sample. Such local anisotropic defect configurations lead to an additional term in the free energy of the phase transition;

$$G = \frac{A}{2}(T - T_C)Q^2 + \frac{B}{4}Q^4 + \frac{C}{6}Q^6 - h_1 Q - h_2 Q^2. \tag{3}$$

Coupling of the form $-h_2 Q^2$, where h_2 is the field (here, the uniform stress of the defects), is always allowed by symmetry; it causes T_C to vary with chemical doping. The term $-h_1 Q$ is not symmetry allowed for the uniform state, but if configurations of defects with the appropriate symmetry are present in the sample then the resulting strains can have the same symmetry as the order parameter and the term is allowed. Physically this could mean that a few Ca atoms together make the octahedra rotate in the same way as happens in the low temperature phase. Although such clusters appear to be thermodynamically unfavourable, given the large repulsive forces noted above, they may exist as a kinetically frozen-in state. This possibility is consistent with the observation that the Ca doping in the $x = 2.3\%$ sample is rather heterogeneous.

Figure 6 shows experimental specific heat for $KMn_{1-x}Ca_xF_3$ with $x = 2.3\%$, and the best-fit curve of a 2–4–6 Landau potential with an additional term $-h_1 Q$. We can observe that the tail is consistent with this thermodynamic model. However, since the Ca distribution is not very uniform, the inhomogeneity can influence the data beyond the $-h_1 Q$ term, so that the graph of figure 6 gives only a qualitative conclusion.

In this study, we have shown that the free energy coefficients for the $Pm3m$–$I4/mcm$ phase transition in the $K(Mn, Ca)F_3$ system vary in a smooth way with composition, and

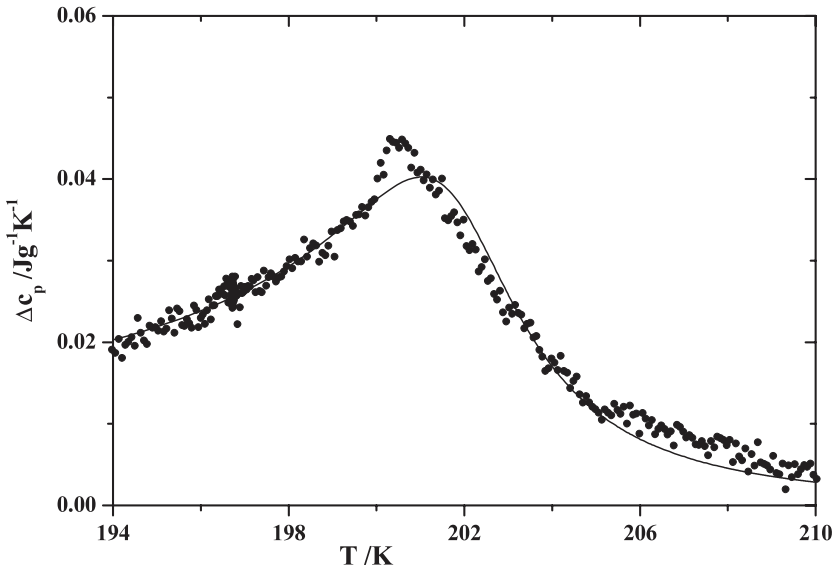

Figure 6. Experimental specific heat for $KMn_{1-x}Ca_xF_3$ with $x = 2.3\%$ and the best-fit curve obtained if a 2–4–6 Landau potential plus the term $-hQ$ is considered.

large changes in the free energy coefficients are only seen for T_C and B. This observation is consistent with a generalized free energy of the form

$$G(T, Q, x) = \frac{A_0}{2}(T - T_{C0})Q^2 + \frac{B_0}{4}Q^4 + \frac{C_0}{6}Q^6 + k_1(x)Q^2 + k_2(x)Q^4, \quad (4)$$

where $k_1(x)$ causes T_C to change as a function of x, and $k_2(x)$ changes B (driving the order of the transition). Although k_1 and k_2 are composition dependent, both functions are highly non-linear, at least for small vales of x.

References

[1] Minkiewicz V J, Fujii Y and Yamada Y 1970 *J. Phys. Soc. Japan* **28** 443
[2] Sakashita H, Ohama N and Okazaki A 1981 *J. Phys. Soc. Japan* **50** 4013
[3] Nicholls U J and Cowley R A 1987 *Phase Transit.* **28** 99
[4] del Cerro J, Romero F J, Gallardo M C, Hayward S A and Jiménez J 2000 *Thermochim. Acta* **343** 89
[5] Hayward S A, Romero F J, Gallardo M C, del Cerro J, Gibaud A and Salje E K H 2000 *J. Phys.: Condens. Matter* **12** 1133
[6] Stokka S, Fossheim K and Samulionis V 1981 *Phys. Rev. Lett.* **47** 1740
[7] Stokka S and Fossheim K 1982 *J. Phys. C: Solid State Phys.* **15** 1161
[8] Buzaré J Y, Fayet J C, Berlinger W and Müller K A 1979 *Phys. Rev. Lett.* **42** 465
[9] Bloch D, Hermann-Ronzaud D, Vettier D, Yelon W B and Alben R 1975 *Phys. Rev. Lett.* **35** 963
[10] Cox U J, Gibaud A and Cowley R A 1987 *Phys. Rev. Lett.* **61** 982
[11] Gibaud A, Shapiro S M, Nouet J and You H 1991 *Phys. Rev.* B **44** 2437
[12] Ratuszna A and Kapusta J 1997 *Phase Transit.* **62** 181
[13] Gibaud A, Cowley R A and Nouet J 1989 *Phase Transit.* **14** 129
[14] Ratuszna A, Pietraszko A, Chelkowski A and Lukaszewicz K 1979 *Phys. Status Solidi* a **54** 739
[15] Ratuzna A, Skrzypek D and Kapusta J 1993 *Phase Transit.* **42** 189
[16] Salje E K H 1995 *Eur. J. Mineral.* **7** 791
[17] Kim Y, Kwun S I, Park S, Oh B and Lee D 1983 *Phys. Rev.* B **28** 3922
[18] Whatmore R, Clarke R and Glazer A M 1978 *J. Phys. C: Solid State Phys.* **11** 3089
[19] Salje E K H, Bismayer U, Wruck B and Hensler J 1991 *Phase Transit.* **35** 61

[20] Hayward S A and Salje E K H 1996 *Am. Mineral.* **81** 1332
[21] Romero F J, Gallardo M C, Jiménez J and del Cerro J 2001 *Thermochim. Acta* **372** 25
[22] Gallardo M C, Romero F J, Hayward S A, Salje E K H and del Cerro J 2000 *Mineral. Mag.* **64** 971
[23] Gallardo M C, Jiménez J and del Cerro J 1995 *Rev. Sci. Instrum.* **66** 5288
[24] del Cerro J 1987 *J. Phys. E: Sci. Instrum.* **20** 609
[25] Jiménez J, Rojas E and Zamora M 1984 *J. Appl. Phys.* **56** 3353
[26] Gallardo M C, Jiménez J, Koralewki M and del Cerro J 1997 *J. Appl. Phys.* **81** 2584
[27] Wruck B, Salje E K H, Zhang M, Abraham T and Bismayer U 1994 *Phase Transit.* **48** 135
[28] Rossetti G A and Navrotsky A 1999 *J. Solid State Chem.* **144** 188
[29] Rios S and Gallardo M C 2000 personal communication